Precipitation Climatology over the Middle East Simulated by the High-Resolution MRI-AGCM3

Akio KITOH* and Osamu ARAKAWA

Meteorological Research Institute
1-1 Nagamine, Tsukuba, Ibaraki 305-0052, Japan
**e-mail: kitoh@mri-jma.go.jp*

Abstract

We investigated the simulation performance of two versions of the atmospheric general circulation model (MRI-AGCM3) in reproducing precipitation climatology over the Middle East in comparison with high-resolution gridded precipitation datasets. Both models overestimated precipitation amounts compared with the observations over this region. The new version, MRI-AGCM3.2, overestimated precipitation much more than the old version, MRI-AGCM3.1, particularly in the winter and spring rainy seasons, but the new version was better than the old version in the summer dry season. We also investigated resolution dependency. The higher the resolution the more the precipitation indicated, but the higher resolution version showed better performance in reproducing the spatial distribution of annual and seasonal mean precipitation, probably due to better representation of orography. These results indicate difficulty in climate model development in terms of regional climate reproducibility.

Key words: high-resolution, Middle East, MRI-AGCM3, precipitation

1. Introduction

The Middle East is located in the Mediterranean climate area with precipitation in winter exceeding that in summer. There is a large north-to-south gradient in precipitation, with desert over the Arabian Peninsula. Figure 1 shows the topography of this region, which is surrounded by the Mediterranean Sea, Black Sea, Caspian Sea, Red Sea and Persian Gulf. Notable mountain ranges are present, such as the Caucasus, Alborz and Zagros Mountains. The Fertile Crescent is a region where ancient civilizations developed. It is located between the Euphrates and Tigris Rivers and is fed by water from mountains to the north. The Taurus Mountains in Turkey form the border of Anatolia with the Mediterranean Sea. There is a north-south oriented narrow range of hills in Lebanon. This topography creates the climatological features of the precipitation distribution in this region.

According to climate-change projections of multiple atmosphere-ocean general circulation models (AOGCMs), the annual precipitation in this region is projected to decrease at the end of the 21st century (IPCC, 2007). However, the horizontal resolution of the climate models used in these projections (between 400 km and 120 km) is not sufficient to resolve the topography well. The increasing ability of computing resources enables us to use climate models with much higher horizontal resolutions. It is anticipated that high-resolution models will simulate orographic precipitation much better than lower-resolution models. Kitoh *et al*. (2008) used a 20-km mesh atmospheric general circulation model (AGCM) to project future streamflows in the "Fertile Crescent" region. Their model has been updated just recently. The new version shows general improvements in simulating heavy monthly-mean precipitation around the tropical Western Pacific, the global distribution of tropical cyclones, the seasonal march of the East Asian summer monsoon, and blockings in the Pacific (Mizuta *et al*., 2012), but an overall assessment of its ability to reproduce regional climates is yet to be addressed. Therefore, validation of the simulated climate is needed in many aspects. In this paper, we compare the precipitation reproducibility of two (old and new) versions of MRI-AGCM. The impact of the horizontal resolution of the model is also investigated, where three versions, *i.e*., 20 km, 60 km and 180 km mesh models, are compared.

2. Data

For model validation, spatially high-resolution observed precipitation data are needed. The main observed dataset used is APHRO_ME1101 (APHRO hereafter), which is daily gridded precipitation for the Middle East, developed by the project of Asian Precipitation - Highly-Resolved Observational Data

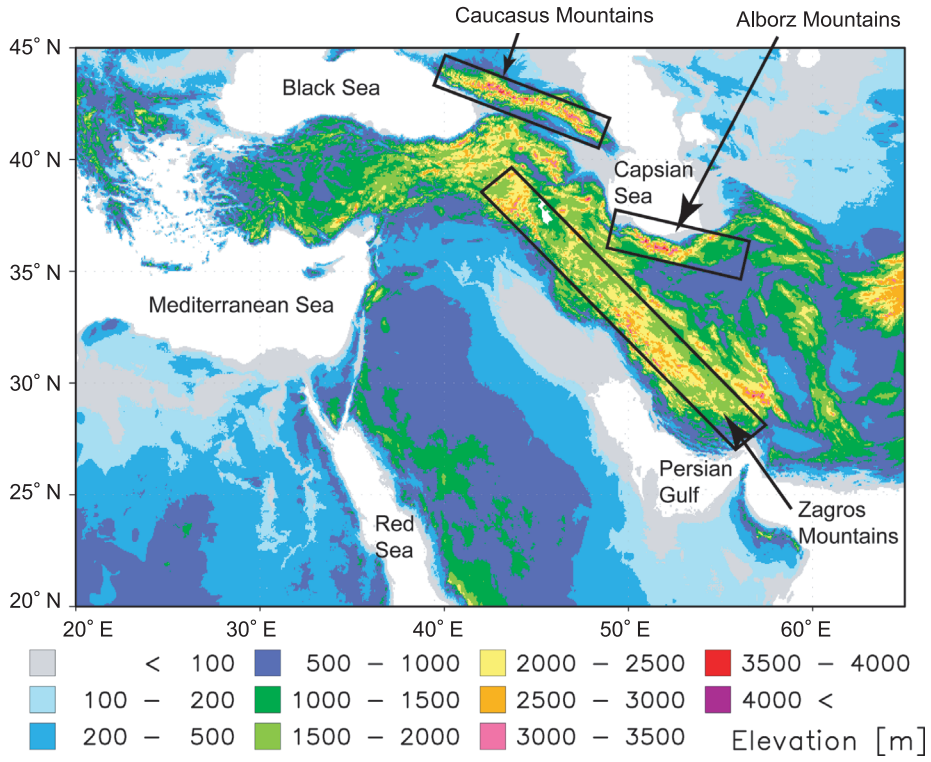

Fig. 1 Topography of the Middle East and surrounding areas. White denotes sea areas.

Integration Towards Evaluation of water resources (APHRODITE) (Yatagai *et al*., 2009). This daily precipitation dataset covers 20°E-65°E, 15°N-45°N with 0.25° resolution during 1951-2007. The APHRO data used in Kitoh *et al*. (2008) (hereafter EM0605) differ from those used in this study. The difference between them comes from differences in (1) the number of station observations, (2) the quality control (QC) system applied to station observations, and (3) the spatial interpolation method. APHRO_ME1101 uses more daily rain gauge observations than EM0605 over Iran, Israel and Saudi Arabia. They are individually collected by the APHRODITE project. In EM0605, QC is manually applied to rain gauge observations (*e.g*., location check). In APHRO_ME1101, an automated objective QC system is utilized (Hamada *et al*., 2011). For spatial interpolation, APHRO_ME1101 uses the Mountain Mapper method (Schaake *et al*., 2004), that spatially interpolates the ratio of precipitation to its climatology. EM0605 uses the Shepard-type method. Other observed data used are CRU_TS2.1 with a 0.5°x0.5° grid from Mitchell and Jones (2005), developed and distributed by the Climatic Research Unit (CRU), University of East Anglia; GPCP_1DD_v1.1 of the Global Precipitation Climatology Project (GPCP) (Huffman & Bolvin, 2009) with a 1.0°x1.0° grid; and the 2.5°x2.5° grid Climate Prediciton Center (CPC) Merged Analysis Precipitation (CMAP) (Xie & Arkin, 1997). APHRO_ME1101 and CRU are based on rain gauges, GPCP is based on satellites, and CMAP uses a combination of rain gauges and satellites.

The GCMs used in this study were MRI-AGCM3.1 and MRI-AGCM3.2, which were jointly developed by the Japan Meteorological Agency (JMA) and the Meteorological Research Institute (MRI). Mizuta *et al*. (2006) described MRI-AGCM3.1, which is based on the operational numerical weather prediction model used at JMA with some modifications added in radiation and land surface processes as a climate model at MRI. The model has a horizontal spectral triangular truncation of spherical function at wave number 959 with a linear grid for wave-to-grid transformation corresponding to about 20 km horizontal grid spacing and has 60 vertical layers with the top at 0.1 hPa. The model has 1,920 longitudinal grids and 960 latitudinal grids over the global domain (there are 242 and 135 grids in the target domain in this paper). The new version, MRI-AGCM3.2, has various new parameterization schemes (Mizuta *et al*., 2012). Improvement in the calculation stability of the semi-Lagrangian scheme enables the time step to be increased from 6 minutes to 10 minutes with this 20-km mesh version. The number of vertical levels has been increased from 60 layers (top at 0.1 hPa) to 64 layers (top at 0.01 hPa) with refinements above the tropopause. A new cumulus parameterization scheme, called the Yoshimura cumulus scheme, has been introduced, where the concepts of both the Arakawa-Schubert-type schemes and Tiedtke-type schemes are incorporated (Yukimoto *et al*., 2011). Both models are simulated for the period from 1979 to 2003 as an Atmospheric Model Intercomparison Project (AMIP)-type experiment where the same observed monthly mean sea surface temperature and sea-ice concentration are prescribed as boundary conditions in both the old and new model experiments. The Hadley Centre Sea Ice and Sea Surface Temperature

data set (HadISST1, Rayner *et al*., 2003) is used. For other specifications, see Mizuta *et al*. (2012). To examine the effect of horizontal resolution, we also performed simulations with lower spatial resolutions, using the same model framework. The resolutions were 60 km (640 longitudinal grids, 320 latitudinal grids), and 180 km (192 and 96 grids).

3. Observations

Figure 2 shows the long-term average annual precipitation for the Middle East region from four observations. The region analysed is 20°E-65°E, 20°N-45°N. In order to make the observation period as even as possible with the model data which are available for 1979-2003, we used APHRO and CMAP covering the 25-year period of 1979-2003, while CRU covers 1979-1998 and GPCP covers 1997-2008, due to data restriction. As our focus in model validation is long-term average precipitation, different data periods do not affect the result.

The APHRO data clearly show a crescent-shaped precipitation belt of more than 500 mm stretching from Israel and southeastern Turkey through the region along the Zagros Mountains. They also show precipitation maxima along the Mediterranean and Black Sea coasts, as well as over the Caucasus Mountains. Precipitation in central Turkey (Anatolia) is around 1 mm/day and is less than that in the coastal areas. There are also precipitation minima over the northwestern part of Iran and over Azerbaijan. A dry area with precipitation less than 100 mm occupies most of the Arabian Peninsula, northern Africa and eastern part of Iran.

The CRU annual precipitation is similar overall to that of APHRO, and shows precipitation maxima along the Mediterranean and Black Sea coasts and over the Caucasus Mountains, along with a minimum over Anatolia. CRU also shows a crescent-shaped precipitation belt, which is not as sharp compared to that of the APHRO data. When compared more precisely with APHRO, the CRU precipitation is less over the crescent area, the Black Sea coast and the southern coast of Caspian Sea. On the other hand, the CRU precipitation is larger than that of APHRO over the Arabian Peninsula. Area averaged annual precipitation for the land region 20°E-65°E, 20°N-45°N is 224 mm in CRU, which is about 20% larger than that of APHRO (179 mm). In short, CRU shows more precipitation than APHRO, while APHRO shows more precipitation over the narrow region of precipitation local maxima.

The horizontal resolution affects the spatial characteristics of precipitation. Therefore, the GPCP and CMAP data do not show detailed structures compared with the previous two datasets. GPCP has a hint of a local maximum along the Zagros Mountains, but fails to show

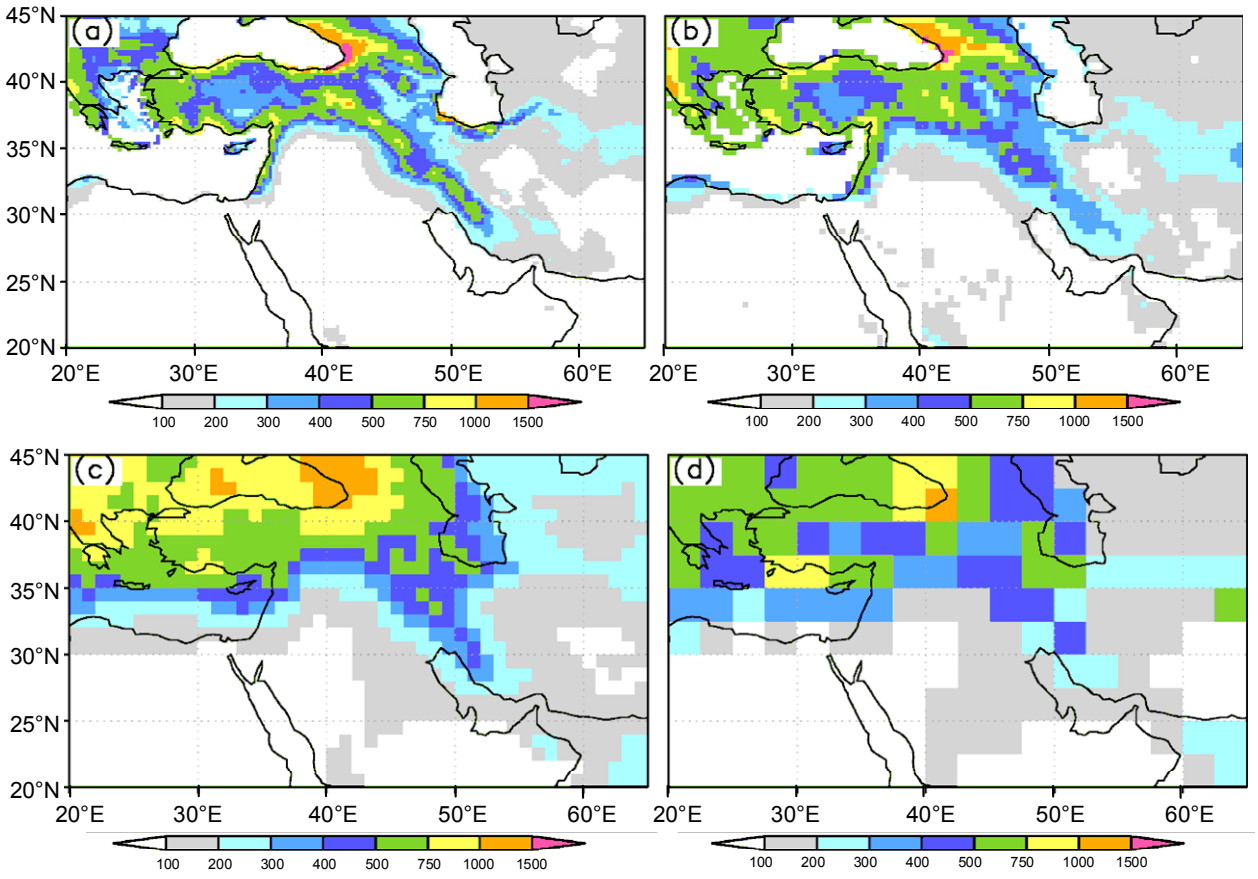

Fig. 2 Observed annual precipitation (mm/year) from four different data sources. (a) APHRO (1979-2003 average), (b) CRU (1979-1998 average), (c) GPCP (1997-2008 average), (d) CMAP (1979-2003 average). (a) and (b) cover land area only.

the local minimum over Anatolia. Both GPCP and CMAP seem to overestimate precipitation over the Arabian Peninsula.

The amounts of precipitation of these four datasets differ sharply. In order to avoid a land-sea mask ambiguity, we calculated the area-average annual precipitation for a 10° by 10° box of 37°E-47°E, 30°N-40°N. It came to 254 mm, 289 mm, 339 mm and 285 mm for APHRO, CRU, GPCP and CMAP, respectively. GPCP showed much larger precipitation amounts in this region. It is noted that the CMAP and CRU estimates were close. APHRO showed the least. GPCP may overestimate precipitation over the analysis region. The smaller area-averaged precipitation in APHRO than in CRU may be associated with APHRO's use of a larger number of rain gauge observations compared with CRU, mainly over Iran.

Figure 3 shows a seasonal breakdown of climatological mean precipitation by APHRO. The area-averaged (20°E-65°E, 20°N-45°N) precipitation is largest in December-February (DJF; 67 mm), followed by March-May (MAM; 56 mm) and September-November (SON; 37 mm), and least in June-August (JJA; 20 mm). Peculiar characteristics found in annual precipitation such as a crescent-shaped precipitation band and maxima along the coasts of the Mediterranean and Black Sea are also seen in DJF, MAM and SON with different magnitudes. When DJF is compared with MAM, there is more precipitation in DJF than in MAM over the coastal region along the Mediterranean and along the northern Persian Gulf. On the other hand, there is more precipitation over the Caucasus Mountains in MAM than in DJF. In JJA, there is a relatively wet region over the Caucasus Mountains. The SON precipitation has similar spatial characteristics to annual precipitation but with slightly less amplitude in daily precipitation.

4. Model Results

Figure 4 shows the annual precipitation simulated by the model in the present-day conditions. Results by MRI-AGCM3.1 and MRI-AGCM3.2 with three different horizontal resolutions are shown. The simulated annual precipitation distribution, particularly by the higher resolution models, reproduces well the one observed by APHRO. Precipitation maxima such as a crescent-type feature along the Zagros Mountains and coastal precipitation along the Mediterranean and Black Sea coasts together with a minimum over Anatolia are all simulated by the 20-km and 60-km mesh models. The 180-km mesh model, however, fails to show the above-mentioned characteristics, except for a broad maximum over the Caucasus Mountains. The new version (MRI-AGCM3.2) clearly shows more precipitation than the old version

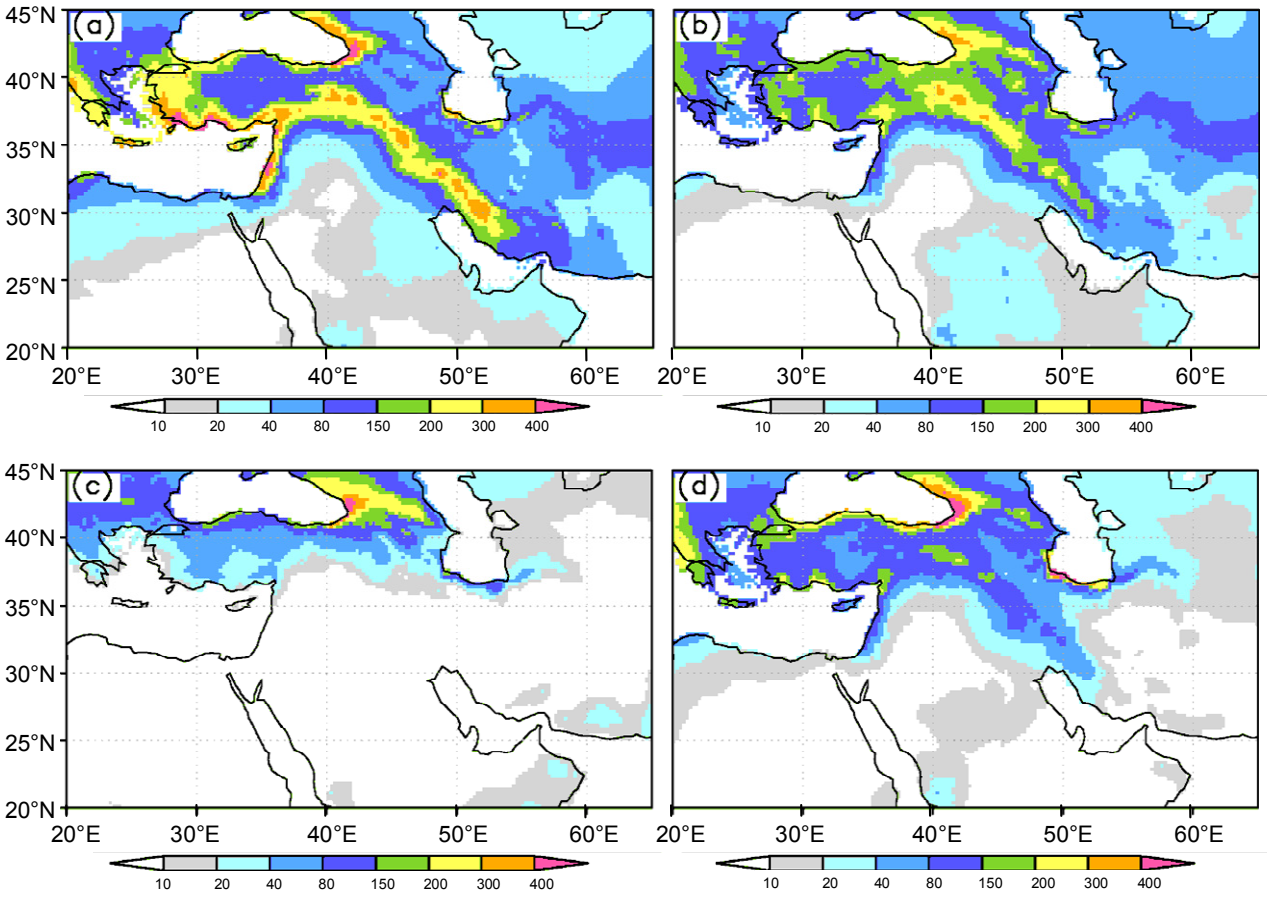

Fig. 3 Observed seasonal precipitation (mm/3months) by APHRO (1979-2003 average). (a) December-February, (b) March-May, (c) June-August, (d) September-November.

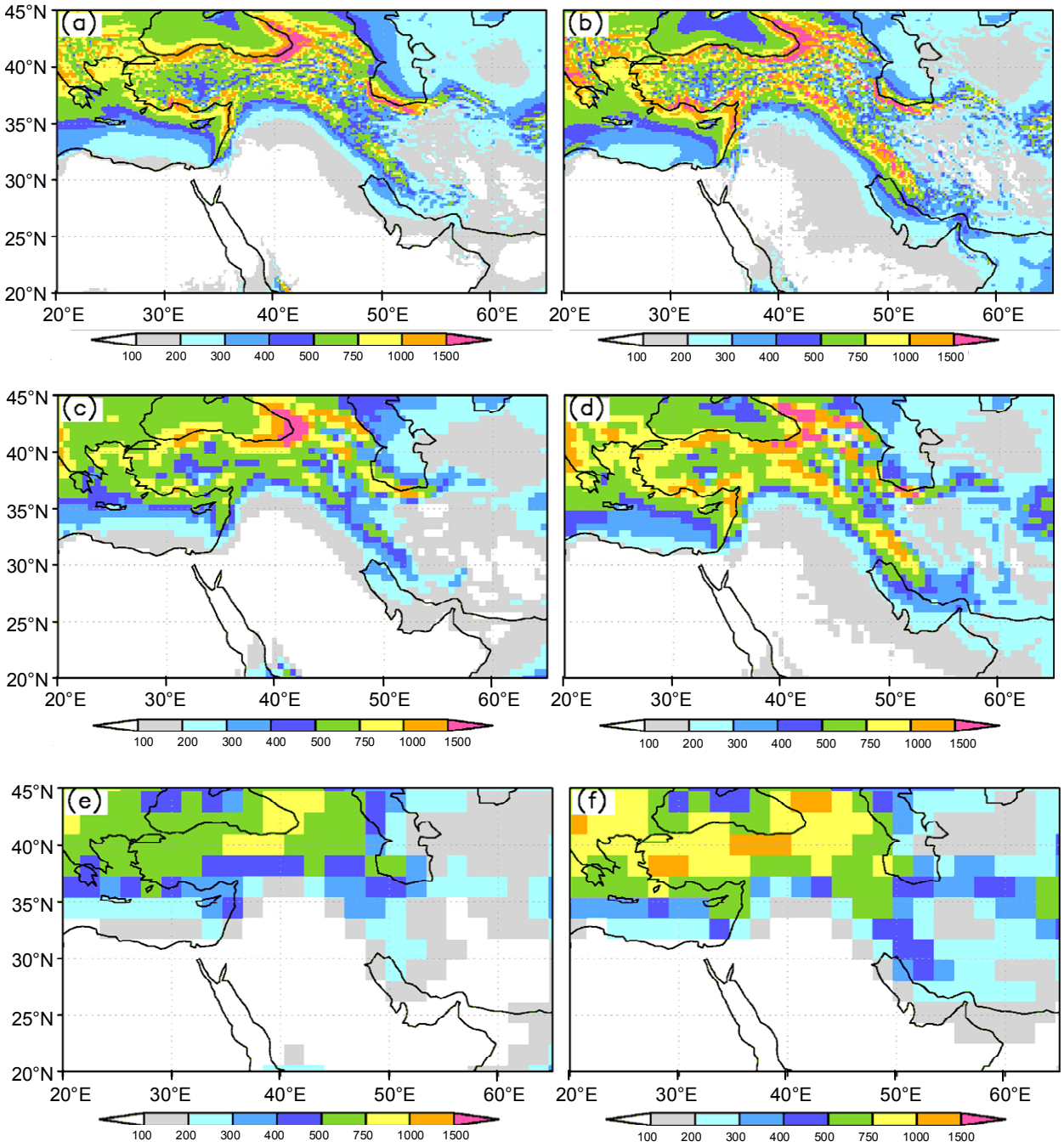

Fig. 4 Simulated annual precipitation (mm/year) for MRI-AGCM3.1 and MRI-AGCM3.2 with three different horizontal resolutions. (a) MRI-AGCM3.1S (20km), (b) MRI-AGCM3.2S (20km), (c) MRI-AGCM3.1H (60km), (d) MRI-AGCM3.2H (60km), (e) MRI-AGCM3.1L (180km), (f) MRI-AGCM3.2L (180km).

(MRI-AGCM3.1) in each resolution category.

Table 1 summarizes the annual and seasonal total precipitation averaged for the land area of the region analysed (20°E-65°E, 20°N-45°N) for the six model versions and two observations (APHRO and CRU). First, it is clear that this model as a whole overestimated the annual and seasonal mean precipitation in this region. Second, there is a resolution dependency with the 20-km mesh model simulating the largest precipitation, the 60-km mesh model the second, and the 180-km mesh model the least within the same model version. Third, MRI-AGCM3.2 generally simulates more precipitation than MRI-AGCM3.1. Therefore, the newer version model actually performs more poorly than the old model compared to APHRO data over the Middle East, and thus the resolution produces a bigger discrepancy in the area-mean precipitation as far as the precipitation amount is concerned. Mizuta *et al*. (2006) showed that the annual global precipitation of MRI-AGCM3.1 overestimated the observations (GPCP and CMAP) by about 15%. The global annual average precipitation rate in MRI-AGCM3.2 is 3.00 mm/day and is about 3% lower than that of MRI-GCM3.1, but still larger than the observed estimate (Mizuta *et al*., 2012). Regionally, they differ by

more than 400 mm in the tropics.

Next we investigated the spatial distribution of climatological mean precipitation. Table 2 shows the pattern correlation coefficients of annual and seasonal mean precipitation distribution between the six model versions and APHRO. Before the calculation, all the data were interpolated into the 60-km mesh grids, and only the land points were used. The higher resolution model better represented the spatial distribution of precipitation than the lower resolution model within the same version of the model. The low-resolution models (180-km mesh models) had a negative bias along the coastal region and over the southern side of the Zagros Mountains, and a positive bias over Anatolia and the northern side of the Zagros Mountains (Fig. 4). These biases decreased as resolution increased. It is noted that the old model (MRI-AGCM3.1) better represents the spatial distribution of precipitation than the new model (MRI-AGCM3.2). In short, the high-resolution model shows better representation of spatial features of annual and seasonal mean precipitation, but with excessive amounts in the region analysed. This caveat becomes larger in the new version of the model. The reason needs to be investigated.

Figure 5 shows the seasonal march of monthly mean precipitation averaged for the land area of the region analysed (20°E-65°E, 20°N-45°N). The two observations (APHRO and CRU) show a similar seasonal march, with double maxima in December and March and minima during July-September. However, they differ quantitatively, with CRU being about 1.2~1.3 times larger than APHRO in all months. The annual mean value from APHRO is 0.49 mm/day, while that from CRU is 0.61 mm/day. The wettest month (December in APHRO, March in CRU) has almost four times the precipitation of the driest month (September in APHRO, August in CRU).

We found that the simulated precipitation has systematic biases compared with the observations. The two model versions show quite different seasonal marches of Middle Eastern precipitation. MRI-AGCM3.1 (Fig. 5a) shows a modest seasonal variation, while MRI-AGCM3.2 (Fig. 5b) shows a distinct seasonal variation. In MRI-AGCM3.1, the amount of wet season precipitation is comparable to the observations, while the dry season precipitation is overestimated, resulting in a smaller contrast of monthly precipitation within a year. It is noted that the higher the resolution, the larger the monthly precipitation in all months. The good performance of area-averaged precipitation in the low resolution model, however, comes from cancellation of model errors: in MAM, the 180-km mesh MRI-AGCM3.1L has a negative bias in the coastal area and over the Zagros Mountains, and a positive bias in Anatolia and the Caucasus Mountains, and they cancel out in the area-averaged precipitation with a false resemblance to the observations. In MRI-AGCM3.2, the dry season precipitation is comparable to the observed estimates, while that of the wet season is highly overestimated by the model. In particular, this model shows excessive precipitation in the MAM season. This overestimation comes mainly

Table 1 Annual and seasonal mean precipitation in mm, averaged, land only of 20°E-65°E, 20°N-45°N. ANN: Annual, DJF: Decmber-February, MAM: March-May, JJA: June-August, SON: September-November.

Data	ANN	DJF	MAM	JJA	SON
APHRO	179	67	56	20	37
CRU	224	75	62	54	52
MRI-AGCM3.1S (20km)	286	91	90	47	58
MRI-AGCM3.2S (20km)	328	106	118	38	67
MRI-AGCM3.1H (60km)	244	79	68	41	56
MRI-AGCM3.2H (60km)	317	105	113	35	63
MRI-AGCM3.1L (180km)	196	67	56	26	47
MRI-AGCM3.2L (180km)	287	95	104	29	58

Table 2 Spatial correlation coefficients of annual and seasonal mean precipitation against APHRO over the land area of 20°E-65°E, 20°N-45°N. ANN: Annual, DJF: Decmber-February, MAM: March-May, JJA: June-August, SON: September-November.

Data	ANN	DJF	MAM	JJA	SON
MRI-AGCM3.1S (20km)	0.872	0.847	0.847	0.848	0.845
MRI-AGCM3.2S (20km)	0.863	0.844	0.846	0.835	0.809
MRI-AGCM3.1H (60km)	0.860	0.818	0.811	0.817	0.854
MRI-AGCM3.2H (60km)	0.842	0.833	0.824	0.811	0.810
MRI-AGCM3.1L (180km)	0.800	0.740	0.774	0.812	0.765
MRI-AGCM3.2L (180km)	0.797	0.758	0.785	0.843	0.746

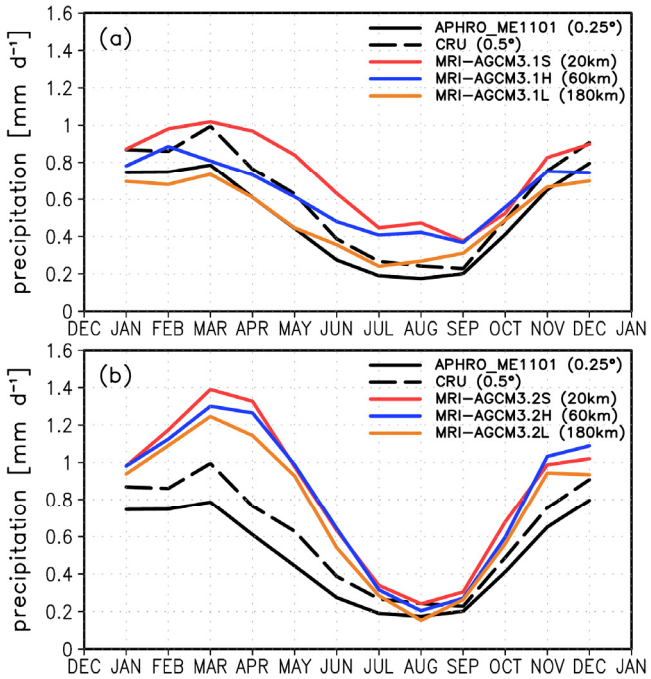

Fig. 5 Seasonal march of land-area averaged monthly mean precipitation (mm/day) for the area analysed (20°E-65°E, 20°N-45°N).
(a) Solid black line: APHRO, dashed black line: CRU, red line: MRI-AGCM3.1S (20km), blue line: MRI-AGCM3.1H (60km), orange line: MRI-AGCM3.1L (180km).
(b) As in (a) except for MRI-AGCM3.2.

from excessive precipitation over the mountainous areas. Again, the higher resolution model tends to show larger precipitation than the lower resolution model throughout the year.

Figure 6 shows the elevation dependency of annual mean terrestrial precipitation over the region of 20°E-65°E, 20°N-45°N. The grids of APHRO include rain gauge observations at all altitudes. It is noted that the spatial distribution of land areas at one altitude in one horizontal resolution is not always identical to that in other horizontal resolutions. The precipitation in two observations (APHRO and CRU) increases with altitude. The precipitation by CRU is greater than that of APHRO at all altitudes, with the difference between them being 0.1-0.2 mm/day. The two model versions show a qualitatively similar elevation dependency but MRI-AGCM3.2 shows more precipitation than MRI-AGCM3.1 at all altitudes. MRI-AGCM3.2 overestimates precipitation at all altitudes compared with the observations. In MRI-AGCM3.1, precipitation increases at all altitudes as horizontal resolution becomes higher. However, in MRI-AGCM3.2, that dependency is not so clear. What the two model versions have in common is that the difference in annual precipitation between high and low altitudes becomes larger when the horizontal resolution is finer. The 180 km and 60 km mesh models tend to show a peak in precipitation rate at some altitude, but the 20 km mesh models show the largest precipitation rate at the highest elevation bin. The APHRO data support the 20 km mesh model results, though the region with elevation higher than 3000 m is very limited, found only within the Caucasus Mountains and the Alborz Mountains (Fig. 1).

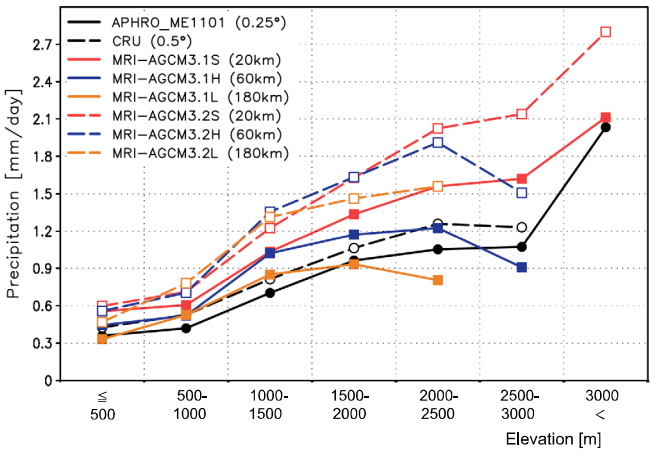

Fig. 6 Elevation dependency of annual mean precipitation intensity (mm/day) for the area analysed (20°E-65°E, 20°N-45°N). Solid black line: APHRO, dashed black line: CRU, solid red line: MRI-AGCM3.1S (20km), solid blue line: MRI-AGCM3.1H (60km), solid orange line: MRI-AGCM3.1L (180km), dashed red line: MRI-AGCM3.2S (20km), dashed blue line: MRI-AGCM 3.2H (60km), dashed orange line: MRI- AGCM3.2L (180km).

5. Concluding Remarks

In this paper, we investigated the precipitation climatology of MRI-AGCM3 over the Middle East against observations. Generally, the models reproduced the regional pattern of precipitation distributions well, but overestimated precipitation amounts compared with the observations. Investigation of resolution dependency among 20, 60 and 180 km mesh models shows that the higher the resolution, the better the performance in capturing the spatial distribution of seasonal and annual mean precipitation in this region, indicating the impact of topography in simulating regional characteristics of climate. At the same time, the higher the resolution, the more the precipitation amount was overestimated, particularly in high mountain regions, probably due to better representation of orography. We also investigated the precipitation climatology of two model versions. The new version, MRI-AGCM3.2, overestimated precipitation much more than the old version, MRI-AGCM3.1, particularly in the winter and spring rainy seasons over the Middle East, while the new version was better than the old version in the summer dry season. The reason for this discrepancy should be investigated for further model development.

Acknowledgements

The APHRODITE's Water Resources project was supported by the Environment Research & Technology Fund of the Ministry of the Environment, Japan. The model development and calculation was conducted under the framework of the “Projection of the change in future weather extremes using super-high-resolution atmospheric models” of the KAKUSHIN Program funded by the Ministry of Education, Culture, Sports, Science and Technology, Japan. The calculations were performed on the Earth Simulator of the Japan Agency for Marine-Earth Science and Technology.

References

Hamada, A., O. Arakawa and A. Yatagai (2011) An automated quality control method for daily rain-gauge data. *Global Environmental Research*, 15: 183-192.

Huffman, G.J. and D.T. Bolvin (2009) GPCP one-degree daily precipitation data set documentation. <ftp://precip.gsfc.nasa.gov/ pub/1dd-v1.1/1DD_v1.1_doc.pdf>

IPCC (2007) *Climate Change 2007: The Physical Science Basis. Contribution of Working Group I to the Fourth Assessment Report of the Intergovernmental Panel on Climate Change*, Cambridge University Press.

Kitoh, A., A. Yatagai and P. Alpert (2008) First super-high-resolution model projection that the ancient "Fertile Crescent" will disappear in this century. *Hydrological Research Letters*, 2: 1-4.

Mitchell, T.D. and P.D. Jones (2005) An improved method of constructing a database of monthly climate observations and associated high-resolution grids. *International Journal of Climatology*, 25: 693-712.

Mizuta, R., K. Oouchi, H. Yoshimura, A. Noda, K. Katayama, S.

Yukimoto, M. Hosaka, S. Kusunoki, H. Kawai and M. Nakagawa (2006) 20-km-mesh global climate simulations using JMA-GSM model: mean climate states. *Journal of the Meteorological Society of Japan*, 84: 165-185.

Mizuta, R., H. Yoshimura, H. Murakami, M. Matsueda, H. Endo, T. Ose, K. Kamiguchi, M. Hosaka, M. Sugi, S. Yukimoto, S. Kusunoki and A. Kitoh (2012) Climate simulations using the improved MRI-AGCM with 20-km grid. *Journal of the Meteorological Society of Japan* (in press).

Rayner, N.A., D.E. Parker, E.B. Horton, C.K. Folland, L.V. Alexander, D.P. Rowell, E.C. Kent and A. Kaplan (2003) Global analyses of sea surface temperature, sea ice, and night marine air temperature since the late nineteenth century. *Journal of Geophysical Research*, 108(D14): 4407, doi:10.1029/2002JD002670.

Schaake, J., A. Henkel and S. Cong (2004) Application of PRISM climatologies for hydrologic modelling and forecasting in the western U.S. *Proceeding of 18th Conference on Hydrology, 84th American Meteorological Society (AMS) Annual Meeting*, Seattle, Washington.

Xie, P.-P. and P.A. Arkin (1997) Global precipitation: A 17-year monthly analysis based on gauge observations, satellite estimates and numerical model outputs. *Bulletin of the American Meteorological Society*, 78: 2539-2558.

Yatagai, A., O. Arakawa, K. Kamiguchi, H. Kawamoto, M.I. Nodzu and A. Hamada (2009) A 44-year daily gridded precipitation dataset for Asia based on a dense network of rain gauges. *Scientific Online Letters on the Atmosphere*, 5: 137-140.

Yukimoto, S., H. Yoshimura, M. Hosaka, T. Sakami, H. Tsujino, M. Hirabara, T.Y. Tanaka, M. Deushi, A. Obata, H. Nakano, Y. Adachi, E. Shindo, S. Yabu, T. Ose and A. Kitoh (2011) Meteorological Research Institute Earth System Model Version 1 (MRI-ESM1): Model Description. *Technical Report of the Meteorological Research Institute*, 64, 83pp. <http://www.mri-jma.go.jp/Publish/Technical/index_en.html>

Akio KITOH

Akio KITOH is Director of the Climate Research Department of the Meteorological Research Institute (MRI), Japan Meteorological Agency (JMA). He has a Doctor of Science degree from Kyoto University. He is leading the projects "Research on Prediction of Climate and Environmental Change to Contribute to Mitigation Plan Decision Making Against Climate Change" funded by the Japan Meteorological Agency (JMA) (FY2010-2014) and "Projection of Change in Future Weather Extremes Using Super-High Resolution Atmospheric Models" funded by the Ministry of Education, Culture, Sports, Science and Technology (MEXT) (FY2007-2011). He was lead author of the IPCC Working Group I Second, Third and Fourth Assessment Reports, and is lead author of the IPCC Working Group I Fifth Assessment Report.

Osamu ARAKAWA

Osamu ARAKAWA is a Research Associate at the Meteorological Research Institute (MRI) of the Japan Meteorological Agency (JMA). He is interested in atmospheric science and climatology. He has used climate models to study climate variations from intra-seasonal to inter-decadal timescales mainly over the tropics.

(Received 26 May 2011, Accepted 7 November 2011)